Hollins University
Hollins Digital Commons

Physics Faculty Scholarship

Physics

2011

MHz Few-body Frequency Shift Detected in a Cold 85Rb Rydberg Gas

Jianing Han
Hollins University

Follow this and additional works at: https://digitalcommons.hollins.edu/physfac

Part of the Physics Commons

MHz few-body frequency shift detected in a cold ^{85}Rb Rydberg gas

Jianing Han

Physics Department, Hollins University, P. O. Box 9707, Roanoke, Virginia 24020, USA and
Department of Physics, University of Virginia, Charlottesville, Virginia 22904, USA

We have observed a density-dependent frequency shift of more than 4 MHz in a cold ^{85}Rb Rydberg gas trapped in a magneto-optical trap. A one-dimensional linearly aligned four-body model is proposed to explain the experimental data, and the calculation matches the experimental data. The calculation also shows that if the energy detuning between the two coupled states, the $nsnsns(n+1)s$ and $nsnsnpnp$ states in this case, is small, the lowest level of the $nsnsnpnp$ manifold has the maximum mixing probability, causing a frequency shift instead of line broadening. The results reported may be used for few-body blockade, Rydberg single-atom imaging, studying few-body to many-body transitions and interactions, and few-body ionization as well as quantum metrology.

I. INTRODUCTION

A cold Rydberg gas demonstrates multipole interactions due to its low temperature and the large dipoles of cold Rydberg atoms. The lowest order interaction is the dipole-dipole interaction. At a small internuclear spacing $R \ll [(r_1 r_2)/\Delta]^{\frac{1}{3}}$, the dipole-dipole interaction is called the first-order dipole-dipole interaction, which has an R^{-3} dependence, where $r_{1,2}$ are the dipole moments and Δ is the energy spacing between two adjacent states. At a large internuclear spacing $R \gg [(r_1 r_2)/\Delta]^{\frac{1}{3}}$, the dipole-dipole interaction is called the van der Waals interaction or the second-order dipole-dipole interaction, which can be solved by second-order perturbation theory.

One of the applications of the dipole-dipole interaction is the dipole blockade; the excitation of one atom suppresses the excitation of neighboring atoms. Dipole blockade was first observed in 1981 [1] and was first proposed as quantum gates by Jaksch *et al.* [2] and then by Lukin *et al.* [3]. Following that, Tong *et al.* [4], Singer *et al.* [5], Cubel Liebisch *et al.* [6], and Heidemann *et al.* [7] experimentally studied the van der Waals blockade using lasers. Vogt *et al.* [8,9] investigated the dipole blockade using electric-field-tuned Förster resonances. Afrousheh *et al.* studied the on-resonance dipole-dipole interaction [10]. However, most of these studies show density broadening, and no frequency shift has ever been observed. Here, I demonstrate that MHz frequency shifts are observed. This frequency shift is the frequency difference between the transition-frequency at a specific internuclear spacing and the transition-frequency at $R \to \infty$. Specifically, microwaves are used as precision probes to detect the strongly coupled states $38s38s38s39s$ and $38s38s38p_{3/2}38p_{3/2}$, which are different in energy by 4.46 MHz at $R \to \infty$. Due to the strong coupling between these two states, one of the energy levels shifts more than 4 MHz at shorter R. The resonance reported here provides an easy means to accurately measure the distance between two Rydberg atoms if only two atoms are addressed and may be employed for quantum computing. More bodies can provide more degrees of freedom in quantum computing, which cannot be produced by two bodies. The frequency-dependent shift can be used to study few-body entanglements as well as quantum metrology through studying the electron interference of the coupled states.

The dipole-blockade studies have previously focused on two bodies. Here the few-body nature of this phenomenon is explored. In a cold Rydberg gas, the interaction regions, one-body→two-body→three-body, can be separated by controlling the atomic density [11]. However, no obvious evidence shows the four-body interaction yet. One way to obtain the three-body to four-body transition is to increase the density or increase the principal quantum number n; however, due to the energy-level structures, more-than-four-body interactions may be involved. The second way of studying the four-body interaction is to study the nearly resonant dipole-dipole coupled states or four-body resonances. Here, I choose one of the nearly resonant dipole-dipole coupled states, $38s38s38s39s$ and $38s38s38p_{3/2}38p_{3/2}$, to study the few-body interaction.

This article is arranged in the following way. The theory is described in the next section followed by the experimental procedures. The MHz frequency shift caused by four-body pairwise dipole-dipole interactions is then demonstrated. I first illustrate more than 4-MHz frequency shifts and then prove that the frequency shifts are due to the fact that the upper level downshifts with increasing densities instead of the upshift of the lower level. Finally, I will show that the shifts are caused by more-than-three-body interactions.

II. THEORY

Here, I first simplify the picture by considering two levels, and the complete calculations are described below. Two close atoms interact through the dipole-dipole-interaction potential

$$V_{12} = \frac{\vec{r}_1 \cdot \vec{r}_2 - 3(\vec{r}_1 \cdot \hat{R})(\vec{r}_2 \cdot \hat{R})}{R^3}, \qquad (1)$$

and the induced frequency shift can be calculated by diagonalizing the matrix composed by the considered state and its nearby state. The two levels repel each other through two-body dipole-dipole interactions. In other words, the upper level shifts up, and the bottom level shifts down relative to the two atomic energy levels. The size of the frequency shift is [12,13]

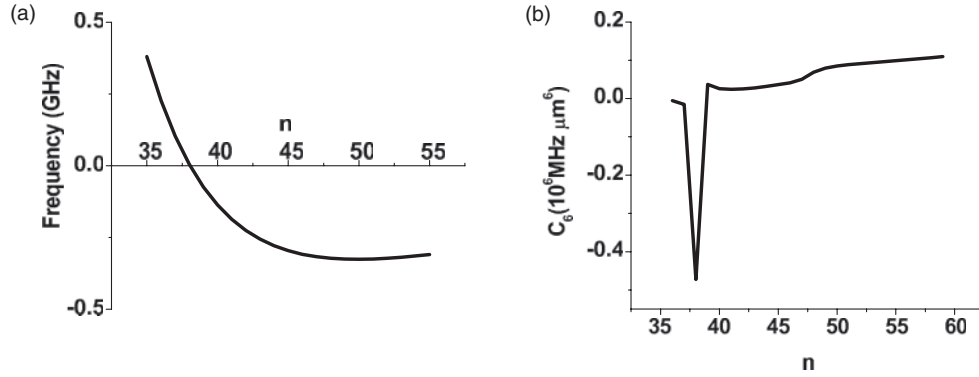$$\frac{V^2}{\Delta} = \frac{C_6}{R^6}, \qquad (2)$$

FIG. 1. (a) The energy difference between $ns(n+1)s$ and $np_{3/2}np_{3/2}$ as a function of the principal quantum number n. (b) C_6 coefficients for the $ns(n+1)s$ states.

where C_6 is the van der Waals coefficient. If we consider two nearby energy levels in a ^{85}Rb gas, the $ns(n+1)s$ state and the $np_{3/2}np_{3/2}$ state, we plot the energy difference Δ between these two as a function of the principal quantum number n as shown in Fig. 1(a). The two energy levels cross at $n \approx 38$. The energy detuning between the $38s39s$ state and the $38p_{3/2}38p_{3/2}$ state is $\Delta \approx 4.46$ MHz. This small detuning results in a large frequency shift as shown by Eq. (2). Figure 1(b) plots C_6 versus the principal quantum number n, showing a maximum at $n = 38$ and indicating the strongest coupling between $38s39s$ and $38p_{3/2}38p_{3/2}$.

The three-body pairwise dipole-dipole-interaction potential is presented in Ref. [11] to explain the high-density data where the spp peak shows broadening to both higher frequencies and lower frequencies. Similar three-atom calculations are conducted for $38s38s39s$ and $38s38p_{3/2}38p_{3/2}$ as shown in Fig. 2(a). The source of the 4.46-MHz splitting at $R = \infty$ in both Figs. 2(a) and 2(b) comes from the energy difference between $38s + 2 \times 38p_{3/2}$ and $2 \times 38s + 39s$ at $R = \infty$. Here, I continue to use the notation used in Ref. [12] for the single-atom system. Specifically, when I write $2 \times 38s + 39s$, it means that the interaction between atoms is negligible,

and $38s38s39s$ means that all three atoms involved interact with each other and that they are coupled through pairwise dipole-dipole interactions. If we start with the $2 \times 38s + 39s$ state at $R = \infty$, there is more and more of the $38s38p_{3/2}38p_{3/2}$ state mixed in the $38s38s39s$ state with decreasing internuclear spacing. According to my calculation, the lowest upper level in Figs. 2(a) and 2(b), the highlighted level, has the maximum mixing probability, more than 90%, compared to the rest of the upper levels. In the following discussion, the shift refers to the shift of this energy level.

To achieve the amount of shift observed experimentally, a shift of more than 4 MHz, the calculated atomic density required by the three-body interaction is 30 times denser than the measured atomic density. The two-dimensional (2D) and 3D three-body calculations cannot fully explain the experimental data either, and the detailed calculations will be presented elsewhere. The conversion between the internuclear spacing and the density can be found in Ref. [14]. I consider four atoms with the nearest-neighbor internuclear spacing R equally distributed along a line as shown in Fig. 3(a), and I assume the atoms' spins are aligned to the internuclear axis. Therefore, the total spin of this system is 2.
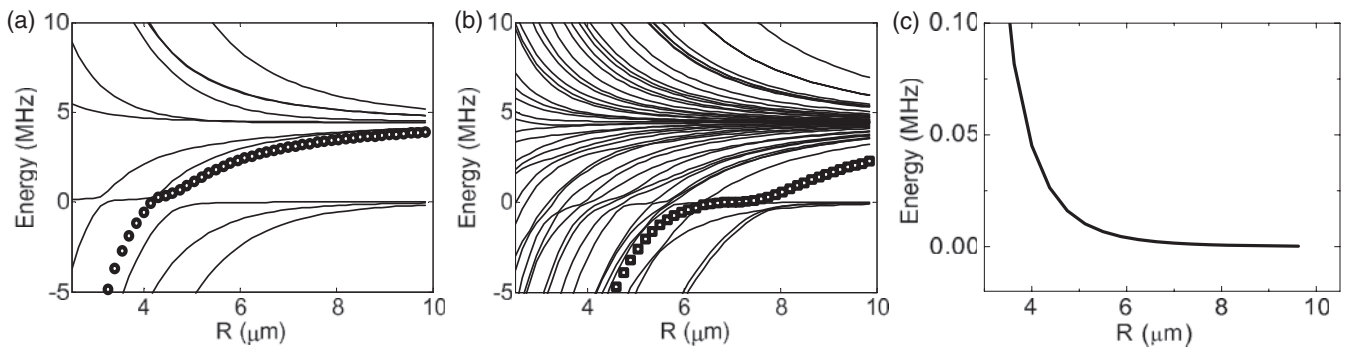

FIG. 2. (a) The energy levels of a 1D three-atom model. The level, which has the maximum population transfer at larger internuclear spacings, is highlighted ($\circ$). The upper nine levels converge to $38s + 2 \times 38p_{3/2}$ at $R \to \infty$, and the lower three levels converge to $2 \times 38s + 39s$ at $R \to \infty$. (b) The energy levels of a 1D four-atom model. The level, which has the maximum population transfer at larger internuclear spacings, is highlighted ($\square$). The upper 48 levels converge to $2 \times 38s + 2 \times 38p_{3/2}$ at $R \to \infty$, and the lower four levels converge to $3 \times 38s + 39s$ at $R \to \infty$. The internuclear spacing R is shown in Fig. 3(a). (c) The energy level of a 1D four-atom model for the $38s38s38s38s$ state as a function of the internuclear spacing R. This energy level is calculated by the four-body pairwise dipole-dipole coupling between $38s38s38s38s$ and $38s38s38p_{3/2}38p_{3/2}$.
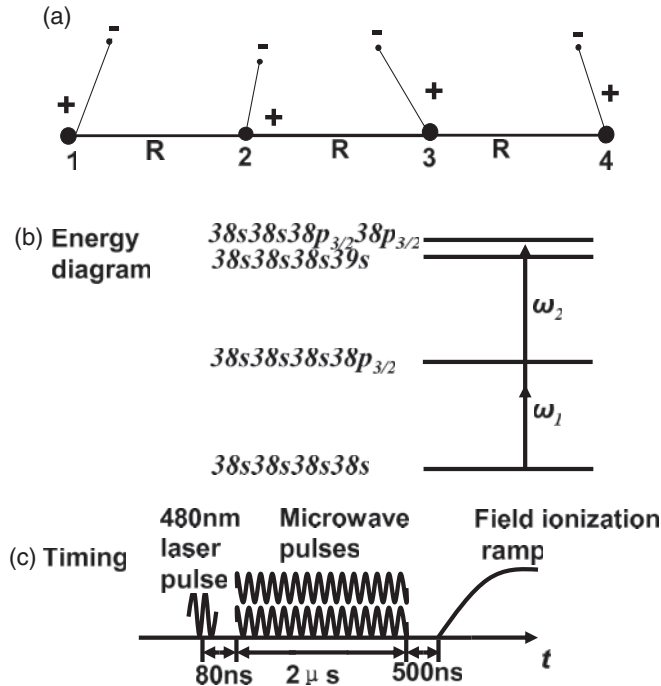
FIG. 3. (a) A 1D four-atom picture. (b) The energy diagram. I set $\omega_1 = 58$ GHz and scan ω_2 around 90 GHz. (c) The sequence of the experiment.

The four-body pairwise dipole-dipole-interaction potential is written as

$$V = \frac{1}{3}(V_{12} + V_{13} + V_{14} + V_{23} + V_{24} + V_{34}). \quad (3)$$

I use similar procedures as reported in Ref. [11]. Here, I use four-body wave functions to construct the interaction Hamiltonian matrix of the potential written in Eq. (3). I again consider the blockaded case in which only one of the four atoms is excited. There are 52 wave functions in total, including four $ssss$ states, $38s38s38s39s$, $38s38s39s38s$, $38s39s38s38s$, and $39s38s38s38s$, and 48 $38s38s38p_{3/2}38p_{3/2}$ states. The calculated results are plotted in Fig. 2(b) and compared with the three-body energy levels. The two highlighted levels in Figs. 2(a) and 2(b) have the maximum transition probability compared to other upper levels. For instance, at the internuclear spacing $R = 7\ \mu$m in Fig. 2(b), the total transition probability to the rest of the $sspp$ levels other than the highlighted level is about 10%, and the total transition probability to the rest of the $sspp$ levels decreases as the internuclear spacing increases. Therefore, the highlighted level using □ represents the experimental observation in the internuclear-spacing range that we are interested in. To have the same frequency shift, for instance, a 4.46-MHz shift, the four-body calculation shows that this happens at 8 μm, and the three-body calculation shows that this happens at 4 μm, requiring an eightfold greater density than that of the four-body case.

III. EXPERIMENT

The experimental apparatus is described in Ref. [15]. Briefly, ^{85}Rb atoms are held in a vapor-cell magneto-optical trap (MOT). The 780-nm trapping lasers establish a population of 10^7 in the $5p_{3/2}$ state as described in other atomic-cooling

literature, and the trap volume of 0.5 mm^3 is midway between two pairs of rods, which serve as field-ionization electrodes and bias-field electrodes. A 480-nm narrow-band ($<$200 MHz) single-mode laser, by frequency doubling and pulse amplifying a 960-nm laser with a 350-mW output from a tapered amplifier seeded by a TOPTICA 110 diode laser, excites the $5p_{3/2}$ atoms to a Rb Rydberg state at a 20-Hz repetition rate. The 480-nm blue laser beam is focused to a FWHM of 0.07 mm to excite the atoms from the $5p_{3/2}5p_{3/2}5p_{3/2}5p_{3/2}$ state to the $38s38s38s38s$ state. The laser's beam width is measured by differentiating the photodiode signal collected behind a razor blade. The total number of atoms is calculated from the oscilloscope signal, which is calibrated by the trap loss in a single laser shot [14]. The density given in this article is the density at the center of the trap or the maximum density [14]. After a delay of 80 ns, two 2-μs microwave pulses are applied to excite the $38s38s38s38s$ state to the $38s38s38p_{3/2}38p_{3/2}$ state. Then, 500 ns after the microwave pulses, a positive field-ionization pulse is applied to two of the four rods to ionize the atoms and pushes the resulting ions toward a detector composed of a pair of microchannel plates. The selective field ionization (SFI), which first separates the atoms and then ionizes them at different fields to separate different states, has been used to resolve different n states [16]. The energy diagram and timing are shown in Figs. 3(b) and 3(c), respectively. The resulting signal is collected by a digitizing oscilloscope and then recorded by a computer.

Two unequal-frequency microwave pulses are employed to avoid the $2 \times 38s$ to $2 \times 38p_{3/2}$ transition. The first frequency, 58 GHz, is generated by an Agilent 83622B sweeper and quadrupoled by a Narda DBS-4060X410. The second frequency is generated by a Hewlett Packard 83620A and doubled first by an active Narda DBS2640X220 doubler and then by a Pacific Millimeter W3WO passive doubler. In the experiment, I keep the 58-GHz microwave fixed and scan the other microwave, $\sim$90 GHz, through the desired transitions. A detailed description of the two-unequal-frequency excitation is given in Ref. [12].

IV. RESULTS AND DISCUSSION

I first show that the $38s38s38p_{3/2}38p_{3/2}$ state can be directly excited from $38s38s38s38s$ by two unequal-frequency photons when the atoms are close. When the atoms are far apart (i.e., $R \to \infty$), the system is essentially a single-atom system. $3 \times 38s + 39s$ and $2 \times 38s + 2 \times 38p_{3/2}$ are the eigenstates of the system, and both are separated by 4.46 MHz. By using two unequal-frequency microwave photons, the population can be transferred to the $3 \times 38s + 39s$ state but not to the $2 \times 38s + 2 \times 38p_{3/2}$ state from the $4 \times 38s$ state because each of the two unequal frequencies does not match with the $38s \to 38p_{3/2}$ transition frequency [12]. However, as the atoms get closer, the $3 \times 38s + 39s$ state is not the eigenstate of the system anymore, and the eigenstate is the superposition of two states, $38s38s38s39s$ and $38s38s38p_{3/2}38p_{3/2}$. Therefore, the $38s38s38p_{3/2}38p_{3/2}$ state mixed in the $38s38s38s39s$ state can be directly excited by two unequal-frequency photons when the atoms are close. A more detailed explanation can be found in Refs. [11,12]. The transition probability and the energy shift of each state relative to its energy at $R \to \infty$ can
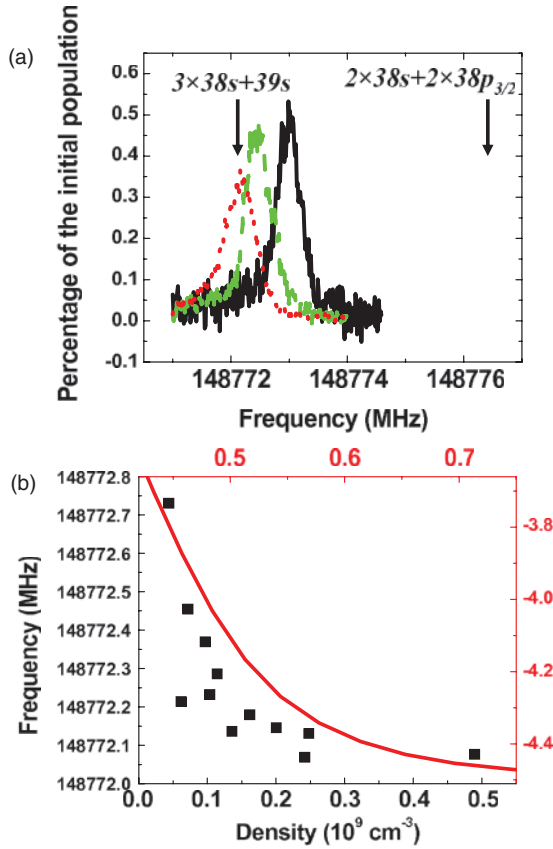
FIG. 4. (Color online) (a) Three microwave scans, from $38s38s38s38s$ to $38s38s38p_{3/2}38p_{3/2}$, measured at three different densities: 6.4×10^7 cm^{-3} (solid black line), 1.6×10^8 cm^{-3} (dashed green line), and 4.8×10^8 cm^{-3} (dotted red line). The arrows indicate the ac-Stark-shifted $4 \times 38s$ to $3 \times 38s + 39s$ and $2 \times 38s + 2 \times 38p_{3/2}$ transition frequencies at $R \to \infty$. The vertical axis is the $38p_{3/2}$ signal over the total Rydberg signal, and the horizontal axis is the sum of the two unequal frequencies. The microwave power is constant for these three scans. (b) The solid red line (-) in the top-right plot is the calculated data from the 1D four-atom model shown as the thicker line in Fig. 2(b). The right-hand-side vertical axis of the top-right plot is the peak frequency shift of the $38s38s38p_{3/2}38p_{3/2}$ state as a function of the Rydberg-atom density. The black squares in the bottom-left plot are the experimental data. The left-hand-side vertical axis of this plot is the transition frequency between $38s38s38p_{3/2}38p_{3/2}$ and $38s38s38s38s$.

be calculated by diagonalizing the matrix composed by the states involved. Here, I simplify the problem by considering two states. A detailed calculation including all states involved, 52 states, is described in the theory section. From these arguments, one would expect that as the density increases, the number of detected $38p_{3/2}$ atoms would increase accordingly as a result of the greater mixing probability. However, due to the dipole-blockade effect, the fractional transfer to the $38s38s38p_{3/2}38p_{3/2}$ state decreases with increasing densities [Fig. 4(a)].

Figure 4(a) shows the number of $38p_{3/2}$ atoms versus the total number of Rydberg atoms as a function of the microwave frequency measured at three different densities with identical microwave powers. I observed that the larger fractional population transfer happens at lower densities.

For instance, about 50% of the population is transferred to $38p_{3/2}$ at the density 6.4×10^7 cm^{-3}. If all the atoms are in $38s38s38p_{3/2}38p_{3/2}$, we expect an equal amount of p and s states to be detected using SFI. According to my calculation, the maximum transition probability, about 90%, to the level plotted by squares in Fig. 2(b) happens at 7 μm, meaning that at least 45% p signal is expected. This is close to my observation of 50% at the density 6.4×10^7 cm^{-3}. At higher densities, less than 45% excitation is observed, indicating a strongly blockaded excitation. More scans are taken at different densities to compare with the calculations; the peak frequencies are plotted in Fig. 4(b).

Not only the excitation suppression is observed as described above, but a frequency shift of more than 4 MHz is also observed. The left arrow in Fig. 4(a) points to the ac-Stark-shifted atomic transition frequency between $38s$ and $39s$, which is lower than the low-density data as shown. The ac-Stark effects will not affect the density effect. To show this, we took a few sets of density measurements at different microwave powers. Similar density-dependent frequency-shift patterns are observed at different microwave powers, so I concluded that the density-dependent frequency shift is due to the dipole-dipole interaction instead of the ac-Stark shift. If we fix the atomic density at the lowest density, measure the transition frequency as a function of the microwave power, and extrapolate the zero-power frequency, this extrapolated zero-power frequency is consistent with the calculated atomic transition frequency between $38s$ and $39s$ calculated with the quantum defects of the s states [15], proving that the lower-density transition frequency is above the atomic transition frequency. In this experiment, the lowest density is achieved by significantly reducing the trapping-laser power. This phenomenon cannot be explained by the two-body picture as described in previous sections [11,12]. The second choice would be the three-body solution, $38s38p_{3/2}38p_{3/2}$ [Fig. 2(a)]. However, the density required to observe a frequency shift of more than 4 MHz of the $38s38p_{3/2}38p_{3/2}$ state is 30 times higher than the actual measured density. Therefore, the three-body picture cannot explain the experimental data.

We introduce the fourth atom, and the calculated energy levels are plotted in Fig. 2(b). I take the empty squares in Fig. 2(b), plot them as a function of the atomic density, and compare them with the measured data as shown in Fig. 4(b). The calculation matches the experimental data, meaning that the peak shift that I observed is the downshift of the upper level with increasing density. Since the upper level $38s38s38p_{3/2}38p_{3/2}$ is 4.46 MHz above the lower level $38s38s38s39s$ at $R \to \infty$, we would expect a frequency-shift range of 0–4.46 MHz (Fig. 2). The reasons for the fact that a smaller frequency-shift range, 3.7–4.46 MHz, is presented in Fig. 4 are as follows. First, the mixing probability of $38s38s38p_{3/2}38p_{3/2}$ in $38s38s38s39s$ is lower at lower densities. For instance, the mixing probability of $38s38s38p_{3/2}38p_{3/2}$ in $38s38s38s39s$ is zero at $R = \infty$. Second, the signal-noise ratio is one of the limiting factors for observing the $38s38s38p_{3/2}38p_{3/2}$ excitation at low densities. Both the measurements and the calculation show a linear dependence, an R^{-3} dependence, at lower densities and are flat at higher densities. With increasing densities, the peaks show more and more asymmetric broadening, and

the center stops moving, which are both consistent with the calculation. In the atomic sample prepared in a MOT, there is a nonuniform-density distribution; however, since the nonuniform-density broadening is less than the Fourier-transform limit of the microwave pulse in the data shown in Fig. 4(a), the nonuniform-density distribution is ignored.

In the experiment, what I measured is the differential frequency shift between $38s38s38s38s$ and $38s38s38p_{3/2}38p_{3/2}$. A broadband laser of 200 MHz was used to excite the $38s$ state, which is weakly coupled with its nearby states. The question is how the shift in $38s38s38s38s$ directly excited from the 200-MHz excitation laser affects the observed spectrum. The four-body pairwise dipole-dipole interaction between two nearest states, $38s38s38s38s$ and $38s38s38p_{3/2}37p_{3/2}$, inducing upshift in frequency on $38s38s38s38s$, is less than 0.05 MHz at 4 μm, and the shift is even smaller at a greater internuclear spacing, which is negligible compared to 4 MHz [Fig. 2(c)].

V. CONCLUSIONS

In conclusion, I have shown that a frequency shift of more than 4 MHz is observed experimentally. Moreover, a 1D four-body model has been introduced to explain the experimental data and is consistent with the measurements. This model shows that what I excited is the $38s38s38p_{3/2}38p_{3/2}$ state mixed in the $38s38s38s39s$ state by pairwise few-body interactions. At higher densities, many-body coupled states may need to be considered. In the future, it would be interesting to study the single-atom imaging of these strongly blockaded states.

ACKNOWLEDGMENTS

[1] J. Raimond, G. Vitrant, and S. Haroche, J. Phys. B **14**, L655 (1981).

[2] D. Jaksch, J. I. Cirac, P. Zoller, S. L. Rolston, R. Cote, and M. D. Lukin, Phys. Rev. Lett. **85**, 2208 (2000).

[3] M. D. Lukin, M. Fleischhauer, R. Cote, L. M. Duan, D. Jaksch, J. I. Cirac, and P. Zoller, Phys. Rev. Lett. **87**, 037901 (2001).

[4] D. Tong, S. M. Farooqi, J. Stanojevic, S. Krishnan, Y. P. Zhang, R. Cote, E. E. Eyler, and P. L. Gould, Phys. Rev. Lett. **93**, 063001 (2004).

[5] K. Singer, M. Reetz-Lamour, T. Amthor, L. G. Marcassa, and M. Weidemuller, Phys. Rev. Lett. **93**, 163001 (2004).

[6] T. Cubel Liebisch, A. Reinhard, P. R. Berman, and G. Raithel, Phys. Rev. Lett. **95**, 253002 (2005).

[7] R. Heidemann, U. Raitzsch, V. Bendkowsky, B. Butscher, R. Low, L. Santos, and T. Pfau, Phys. Rev. Lett. **99**, 163601 (2007).

[8] T. Vogt, M. Viteau, J. Zhao, A. Chotia, D. Comparat, and P. Pillet, Phys. Rev. Lett. **97**, 083003 (2006).

[9] T. Vogt, M. Viteau, A. Chotia, J. Zhao, D. Comparat, and P. Pillet, Phys. Rev. Lett. **99**, 073002 (2007).

[10] K. Afrousheh, K. Afrousheh, P. Bohlouli-Zanjani, D. Vagale, A. Mugford, M. Fedorov, and J. D. D. Martin, Phys. Rev. Lett. **93**, 233001 (2004).

[11] J. Han, Phys. Rev. A **82**, 052501 (2010).

[12] J. Han, J. Phys. B **43**, 235205 (2010).

[13] J. Han, Ph.D. thesis, University of Virginia, 2009 (unpublished).

[14] J. Han and T. F. Gallagher, Phys. Rev. A **79**, 053409 (2009).

[15] W. Li, I. Mourachko, M. W. Noel, and T. F. Gallagher, Phys. Rev. A **67**, 052502 (2003).

[16] T. F. Gallagher, L. M. Humphrey, W. E. Cooke, R. M. Hill, and S. A. Edelstein, Phys. Rev. A **16**, 1098 (1977).